Electronic structures of superlattices under in-plane magnetic field

Jian-Bai Xia and Wei-Jun Fan
Chinese Center of Advanced Science and Technology (World Laboratory), Beijing, China
and Institute of Semiconductors, Chinese Academy of Sciences, P.O. Box 912, Beijing 100083, China
(Received 21 March 1989; revised manuscript received 7 June 1989)

The electronic structures of superlattices under an in-plane magnetic field are studied by the method of expansion with sine functions. The electronic and hole magnetic energy levels are obtained as functions of k_x, k_y and the intensity of the magnetic field. The density of states and the magnetic-optical transition matrix elements are discussed. The variations of the binding energy of the heavy- and light-hole magnetic excitons with the magnetic field and the well width are also obtained. Finally, the electronic energy levels in the magnetic field along an arbitrary direction in the *yz* plane are calculated.

I. INTRODUCTION

The electronic structures and the exciton states in superlattices in the magnetic field perpendicular to the interface have been investigated in many experimental and theoretical works.[1-8] In this case the cyclotron motion of electrons is in the plane of the superlattice parallel to the interface. The quantizations caused by the magnetic field and the confinement of electrons in the growth direction are independent, and the electronic magnetic energy levels in superlattices are relatively simple. The hole magnetic energy levels are more complicated because of the coupling between the heavy and light holes.[6] When the magnetic field is in the direction parallel to the interface, the electronic cyclotron motion is in the growth direction and the quantizations caused by the magnetic field and the confinement of electrons overlap so that the resultant quantum energy levels are determined by the magnitudes of the magnetic field and the quantum well. This will produce a series of interesting physical phenomena.

Experimentally, there have been Shubnikov–de Haas magnetic-resistance measurements by Chang *et al.*[9,10] and magnetic-optical measurements by Belle *et al.*[11] and Raynolds *et al.*[12] In the magnetic-resistance experiments[9,10] the effect of the parallel magnetic field on the quantum oscillations has been observed. Ando[13] first calculated the electronic quantum energy levels of superlattices in the parallel magnetic field for explaining the experiment. Maan[14,15] calculated and analyzed the quantum magnetic energy levels and compared them with the magnetic-optical experiment.[11] The recent magnetic-optical experiment[12] measured the diamagnetic energy shifts of heavy- and light-hole excitons as functions of well width and magnetic field intensity. Lebens *et al.*[16] studied the effect of a parallel magnetic field on tunneling in heterostructures. Recently, Oliveira *et al.*[17] calculated the electronic energy levels in *n*-type modulation-doped quantum wells by a self-consistent method. Fasolino *et al.*[18] and Altarelli *et al.*[19] extended the calculation to the hole magnetic energy levels. They calculated the special case of the component of wave vector along the direction of magnetic field equal to zero.

In this paper we shall use an expansion method with sine functions to study the electronic structures of superlattices in the parallel magnetic field. In Sec. II we present the calculation method and the electronic magnetic energy levels. In Sec. III we discuss the hole magnetic energy levels, in Sec. IV the binding energy of magnetic excitons, and in Sec. V the electronic energy levels of superlattices in the magnetic field along an arbitrary direction between the parallel and perpendicular directions.

II. CALCULATION METHOD AND ELECTRONIC MAGNETIC ENERGY LEVELS

In the following we shall assume that the growth direction of the superlattices is in the z direction, and the magnetic field is in the y direction. Let the vector potential of the magnetic field be

$$\mathbf{A}=(Bz,0,0)\ . \tag{1}$$

The electronic wave function can be written as

$$\psi(\mathbf{r})=e^{ik_x x+ik_y y}\varphi(z)\ , \tag{2}$$

where $\varphi(z)$ satisfies the equation

$$\left[\frac{1}{2m^*}[p_z^2+\beta^2(z+z_0)^2]+V(z)\right]\varphi(z) = \left[E-\frac{\hbar^2k_y^2}{2m^*}\right]\varphi(z)\ , \tag{3}$$

where

$$\beta=\frac{eB}{c}\ , \tag{4}$$

$$z_0=\frac{\hbar k_x}{\beta}\ . \tag{5}$$

$V(z)$ is the potential of the superlattices.

From Eq. (3) we see that the effect of the magnetic field on electrons is equivalent to addition of a parabolic potential, whose origin is at the center of a potential well for $k_x=0$. If we do not consider the superlattice potential $V(z)$ at the moment the quantum energy levels become Landau energy levels, the corresponding wave functions will be the harmonic-oscillator wave functions. The cyclotron-orbit radius depends on the magnetic field B and Landau quantum number n as

$$R_n=\left[(2n+1)\left[\frac{\hbar c}{eB}\right]\right]^{1/2}. \tag{6}$$

Beyond the range of R_n, the wave function vanishes. Thus we take a large L so that $L\gg 2R_n$ for certain $n<N$, and expand the wave function $\varphi(z)$ in terms of sine functions,

$$\varphi(z)=\left[\frac{2}{L}\right]^{1/2}\sum_{m=1}^{\infty}c_m\sin\left[\frac{m\pi z}{L}+\frac{m\pi}{2}\right], \tag{7}$$

which vanishes at $z=-L/2$ and $L/2$. Inserting Eq. (7) into Eq. (3) with $V(z)=0$ and $k_x=k_y=0$, we can obtain accurate Landau energy levels and corresponding wave functions, depending on L and the number of expansion terms in Eq. (7). For example, in the magnetic field $B=10$ T and $m^*=0.067m_0$, if we take $L=1000$ Å and the number of expansion terms $M=40$, we can obtain 15 accurate Landau energy levels with energy $E_{14}=251$ meV; if $L=2000$ Å and $M=80$, we obtain 45 accurate Landau energy levels with $E_{44}=770$ meV.

Then, we consider the superlattice potential $V(z)$. For each $V(z)$ and B, we choose L and M so that the highest accurate Landau energy level is much higher than the quantum energy levels of the superlattice without magnetic field. In this case the $V(z)$ can be considered perturbation, and the convergent quantum energy levels can be obtained with wave functions (7). For the superlattices GaAs-$Al_{0.2}Ga_{0.8}As$, the conduction-band offset is 150 meV, which is much smaller than the Landau energy level $E_{44}=770$ meV in $B=10$ T; thus, taking $L=2000$ Å and $M=80$ is enough to obtain the convergent quantum energy levels. It is noticed from Eq. (6) that $L\propto 1/\sqrt{B}$.

In this paper we shall calculate the magnetic energy levels of the superlattice GaAs-$Al_{0.2}Ga_{0.8}As$; the energy-band parameters used in the calculation are the electronic effective mass $m^*=0.067m_0$, the Luttinger parameters[20] of the valence band, $\gamma_1=6.85$, $\gamma_2=2.1$, $\gamma_3=2.9$, $\kappa=1.2$, and $q=0$,[21] the band offset of the conduction and valence bands, $\Delta V_e=150$ meV and $\Delta V_h=100$ meV, and the widths of the potential well and the potential barrier, 100 and 50 Å respectively.

Figure 1 shows the electronic magnetic energy levels as functions of z_0 for a magnetic field of 10 T. From Fig. 1 we see that there are two kinds of quantum energy levels: one is relatively "flat" and independent of z_0, such as the energy levels at 30 and 110 meV. They are associated with the quantum energy levels in the superlattice without magnetic field. The other type has larger energy dispersion with z_0, and are associated with the parabolic potential arising from the magnetic field.

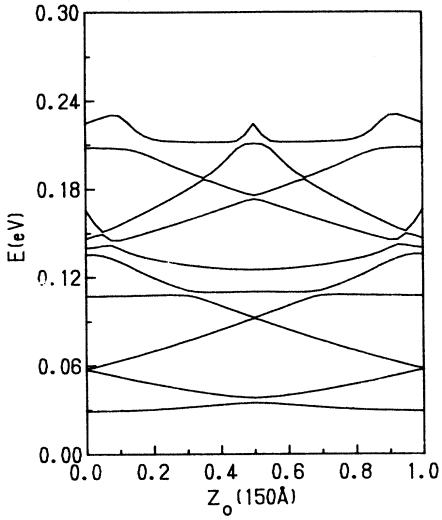

FIG. 1. Electronic magnetic energy levels as functions of z_0 for a magnetic field of 10 T.

Figure 2 shows the variations of magnetic energy levels ($z_0=0$) with the magnetic field. From Fig. 2 we see that most of the energy levels rise quadratically with magnetic field. The energy levels associated with the energy levels in the superlattice without magnetic field, including the ground state, increase slightly with magnetic field.

In order to calculate the density of states, we define the electronic energy as approximately

$$E=E_n-E_{n0}\cos\frac{2\pi z_0}{l}+\frac{\hbar^2k_y^2}{2m^*}, \tag{8}$$

where the second term represents the energy dispersion with z_0 (k_x), which is a periodic function of the superlattice period l. From Eq. (8) we obtained the density of states of the nth energy band,

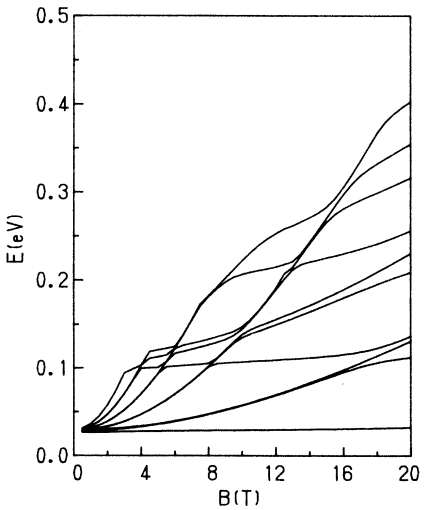

FIG. 2. Variation of the electronic magnetic energy levels ($z_0=0$) with intensity of the magnetic field.

$$n(E)=\begin{cases}\dfrac{1}{\pi^3\hbar^2}\dfrac{eB}{c}\left[\dfrac{2m^*}{E-E_n+E_{n0}}\right]^{1/2}K\left[\left[\dfrac{2E_{n0}}{E-E_n+E_{n0}}\right]^{1/2}\right], & E>E_n+E_{n0}\\ \dfrac{1}{\pi^3\hbar^2}\dfrac{eB}{c}\left[\dfrac{m^*}{E_{n0}}\right]K\left[\left[\dfrac{E-E_n+E_{n0}}{2E_{n0}}\right]^{1/2}\right], & E_n-E_{n0}\le E<E_n+E_{n0}\end{cases} \tag{9}$$

where $K(x)$ is the complete elliptic integral of the first kind, which diverges at $x=1$. Hence the density of states (9) diverges at $E=E_n+E_{n0}$. The variation of $n(E)$ with E is shown in Fig. 3. For $E<E_n+E_{n0}$ the density of states has a step form like the two-dimensional density of states, and for $E>E_n+E_{n0}$ it decreases as $1/\sqrt{E}$, like the one-dimensional density of states. The sharp peak in the density of states is the character of a two-dimensional energy band at the saddle critical point $z_0=l/2(k_x=\beta 1/2\hbar)$ and $k_y=0$, as discussed by Van Hove.[22] If E_{n0} approaches zero, the density of states will be reduced to the one-dimensional density of states,

$$n(E)=\frac{1}{2\pi^2\hbar^2}\frac{eB}{c}\left[\frac{2m^*}{E-E_n}\right]^{1/2},\quad E>E_n\ . \tag{10}$$

Therefore, in the case of the parallel magnetic field the magnetic-optical spectra will exhibit complicated character of both two- and one-dimensional densities of states.

III. HOLE MAGNETIC ENERGY LEVELS

Transforming the coordinate system (x,y,z) in the Luttinger Hamiltonian[20] of the hole in the magnetic field to the new coordinate system (z,x,y), the hole Hamiltonian can be written as

$$H=\frac{1}{2m_0}\begin{bmatrix}P_1+3\hbar\beta\kappa & Q & R & 0\\ Q^* & P_2+\hbar\beta\kappa & 0 & R\\ R^* & 0 & P_2-\hbar\beta\kappa & -Q\\ 0 & R^* & -Q^* & P_1-3\hbar\beta\kappa\end{bmatrix}, \tag{11}$$

where

$$\begin{aligned}P_1&=(\gamma_1+\gamma_2)[p_z^2+\beta^2(z+z_0)^2]\\&\quad+(\gamma_1-2\gamma_2)\hbar^2k_y^2\ ,\\ P_2&=(\gamma_1-\gamma_2)[p_z^2+\beta^2(z+z_0)^2]\\&\quad+(\gamma_1+2\gamma_2)\hbar^2k_y^2\ ,\\ Q&=-2\sqrt{3}\gamma_3\hbar k_y[ip_z+\beta(z+z_0)]\ ,\\ R&=\sqrt{3}\{\gamma_2[p_z^2-\beta^2(z+z_0)^2]\\&\quad-2\gamma_3[\beta(z+z_0)ip_z]-\gamma_3\hbar\beta\}\ .\end{aligned} \tag{12}$$

In deriving Eq. (11), we have assumed that $q=0$ and the hole wave function to be

$$\psi(\mathbf{r})=\begin{bmatrix}\varphi_1(z)\\ \varphi_2(z)\\ \varphi_3(z)\\ \varphi_4(4)\end{bmatrix}e^{ik_xx+ik_yy}\ . \tag{13}$$

As in the case of the electron [Eq. (7)], we expand each $\varphi_j(z)$ in Eq. (13) with sine functions, and thus the hole magnetic energy levels can be obtained.

Figure 4 shows the hole magnetic energy levels as functions of z_0 for a magnetic field of 10 T. From Fig. 4 we see that, similar to the electronic magnetic energy levels, there are two kinds of energy levels: one is relatively flat and associated with the hole energy levels without magnetic field. In Fig. 4 the lowest and excited energy levels (7 and 19 meV) are associated with the heavy- light-hole energy levels (6.85 and 18.2 meV), respectively. The other type of energy level has larger energy dispersion with z_0.

We also calculated the dispersion of the subbands along the k_y direction ($z_0=0$) for a magnetic field of 10 T; the results are shown in Fig. 5. From Fig. 5 we see that, as k_y is larger than $2\pi/l$ (l is the period of the superlattice), the subbands approach parabolic bands, and, as k_y is smaller than $2\pi/l$, there is strong interaction between subbands, and the hybrid bands are formed.

Figure 6 shows the variations of hole magnetic energy levels ($z_0=0$ and $k_y=0$) with magnetic field. For clarity

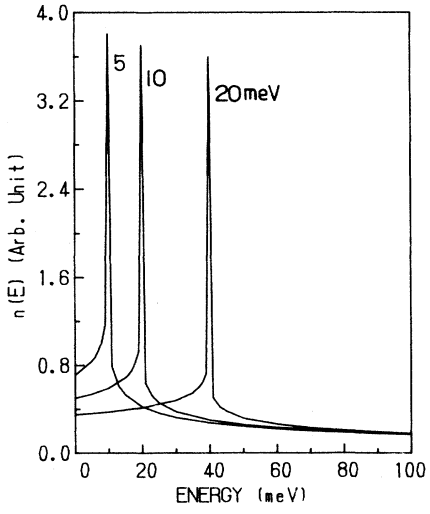

FIG. 3. Density of states of the electronic magnetic subbands for three values of E_{n0} (defined in the text).

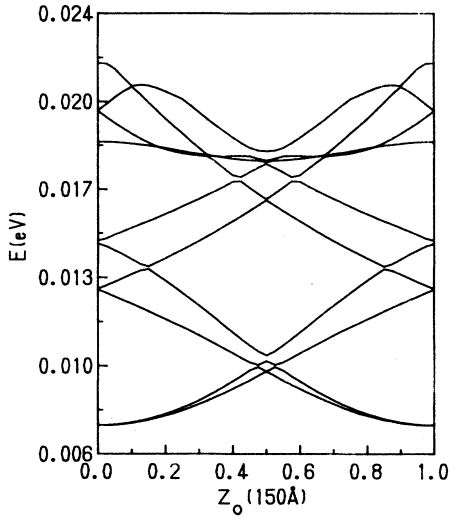

FIG. 4. Hole magnetic energy levels as functions of z_0 for a magnetic field of 10 T.

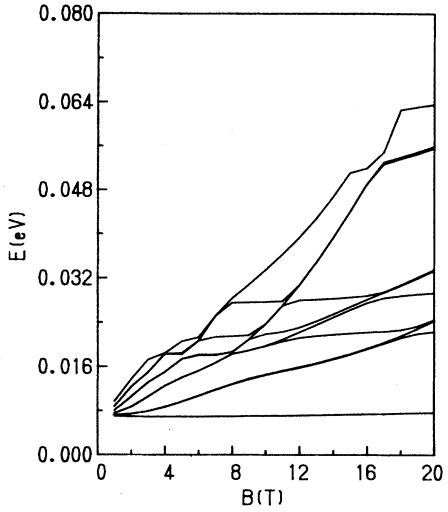

FIG. 6. Variation of the hole magnetic energy levels ($k_x=k_y=0$) of the group $J_y=\frac{3}{2},-\frac{1}{2}$ with magnetic field.

only one group of energy levels $J_y=\frac{3}{2},-\frac{1}{2}$) is shown. From Fig. 6 we see that the hole magnetic energy levels rise (actually descend) quadratically with magnetic field, except for the ground state and the excited states associated with the heavy- and light-hole quantum states without magnetic field.

Having known the electronic and hole energy levels and corresponding wave functions, we can calculate the optical transition matrix elements. According to the effective-mass theory, the true electronic and hole wave functions should be Eq. (2) multiplied by the wave function of the conduction-band bottom, $u_\sigma(\mathbf{r})$ ($\sigma=\pm$), and Eq. (13) multiplied by that of the valence-band top, $u_j(\mathbf{r})$ ($j=\frac{3}{2},\frac{1}{2},-\frac{1}{2},-\frac{3}{2}$), respectively, where σ is the spin component and j is the component of the angular momentum $J=\frac{3}{2}$. The squared optical transition matrix element is

$$Q_{nn'}=\frac{2}{m_0}|\hat{\epsilon}\cdot\langle\psi_e|\mathbf{p}|\psi_h\rangle|^2 , \tag{14}$$

where $\hat{\epsilon}$ is the unit vector of the electric field direction. For the electric field polarizations $\epsilon_+=\epsilon_z+i\epsilon_x$, $\epsilon_-=\epsilon_z-i\epsilon_x$, and ϵ_y, it can be proved that

$$\begin{aligned}
Q_{nn'}(\epsilon_+)&=\frac{2P^2}{m_0}[(\langle\varphi_e|\varphi_{h4}\rangle)^2+\tfrac{1}{3}(\langle\varphi_e|\varphi_{h3}\rangle)^2] ,\\
Q_{nn'}(\epsilon_-)&=\frac{2P^2}{m_0}[(\langle\varphi_e|\varphi_{h1}\rangle)^2+\tfrac{1}{3}(\langle\varphi_e|\varphi_{h2}\rangle)^2] ,\\
Q_{nn'}(\epsilon_y)&=\frac{2P^2}{m_0}\tfrac{2}{3}[(\langle\varphi_e|\varphi_{h2}\rangle)^2+(\langle\varphi_e|\varphi_{h3}\rangle)^2] ,
\end{aligned} \tag{15}$$

where φ_e and φ_{hj} are the electronic and hole wave functions in Eqs. (3) and (13), respectively. $P=\langle s|p_x|X\rangle$; S and X are the orbital wave functions of the crystal conduction-band bottom and valence-band top, respectively.

Table I gives the squared optical transition matrix elements at $k_x=k_y=0$ for a magnetic field of 10 T, taking $2P^2/m_0=18.71$ eV.[6] For clarity, only Q larger than 2 eV are listed in the table. From the table we see that there are two kinds of transitions: one has comparable intensities for polarizations ϵ_+ (or ϵ_-) and ϵ_y. The other only has strong intensity for polarization ϵ_+ (or ϵ_-), but weak intensity for ϵ_y. The former are transitions to heavy-hole states and the latter are transitions to light-hole states. It is noticed that in the case of perpendicular magnetic field the transitions to light-hole states are only of polarization ϵ_z (polarization in the direction of the magnetic field). Therefore, by means of the transitions of

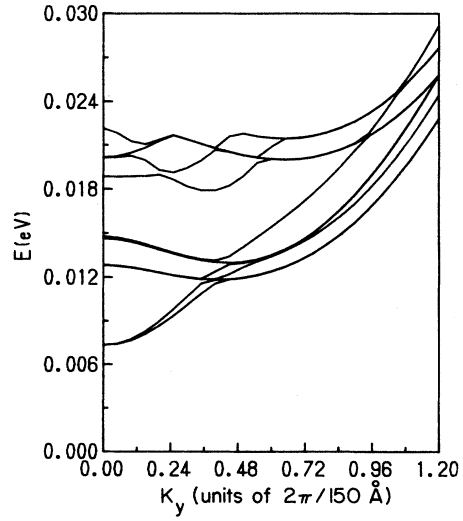

FIG. 5. Hole magnetic energy levels ($z_0=0$) as functions of k_y for a magnetic field of 10 T.

TABLE I. Squared magnetic-optical transition matrix elements (in units of eV). The energy (in parentheses, in units of meV) is given for each energy level. a and b represent the two groups of the hole energy levels. $+$, $-$, and y represent the electric field polarizations ϵ_+, ϵ_-, and ϵ_y, respectively.

			Conduction n		
			1	2	3
	Valence n		(29.36)	(57.44)	(58.01)
b	1	(7.17)	4.749 (+) 4.411 (−) 9.363 (y)		
a	2	(7.17)	4.682 (+) 3.934 (−) 8.822 (y)		
b	3	(12.71)		5.162 (−) 10.324 (y)	
b	4	(12.75)			5.195 (−) 10.389 (y)
a	5	(14.58)			4.738 (+) 9.477 (y)
a	6	(14.70)		4.836 (+) 9.673 (y)	
b	7	(18.75)	13.483 (+) 2.958 (y)		
a	8	(20.03)			8.975 (−)
a	9	(20.04)		8.864 (−)	
a	10	(21.97)	13.447 (−) 2.43 (y)		
b	11	(22.50)			
b	12	(22.55)			
b	13	(22.93)		8.942 (+)	
b	14	(23.27)			9.025 (+)

different polarization, we can distinguish the transitions to heavy- or to light-hole states. The letters a and b in Table I represent two groups of hole energy levels at $k_y=0$, corresponding to $J_y=\frac{3}{2},-\frac{1}{2}$ and $J_y=\frac{1}{2},-\frac{3}{2}$, respectively. Except for the ground states, the electric field polarizations are different for transitions to the states of a and b groups: for heavy-hole states they are ϵ_+ and ϵ_- and for light-hole states they are ϵ_- and ϵ_+, respectively.

IV. MAGNETIC EXCITONS IN SUPERLATTICES

In the case of perpendicular magnetic field, there has been much work on the magnetic exciton.[1,3,7,8] However, in the case of the parallel magnetic field there seems to be no work on the magnetic exciton. Here we use a method similar to that of Greene and Bajaj,[1] assuming the exciton wave function as follows,

$$\psi_{\rm ex}=\varphi_e(z_e)\varphi_h(z_h)G(\rho,z)\ , \tag{16}$$

where $\varphi_e(z_e)$ and $\varphi_h(z_h)$ are the electron and hole wave functions at $k_x=k_y=0$, and $G(\rho,z)$ is the exciton envelope function. ρ,z are the components of the relative coordinate $\mathbf{r}=\mathbf{r}_e-\mathbf{r}_h$ in the xy plane and z direction, respectively. The exciton Hamiltonian is

$$H_{\rm ex}=H_e+H_h-\frac{e^2}{\varepsilon r}\ , \tag{17}$$

where H_e and H_h are the Hamiltonian of electron and hole in the superlattice, respectively.

We further simplify the hole wave function $\varphi_h(z_h)$. The calculation found that for the ground states of the heavy and light hole (the first and second and seventh and tenth states in Table I), the hole density distribution function calculated from Eq. (13) is nearly the same as that calculated with a simple parabolic model, in which the heavy and light holes have the effective mass

$$m_h^*=\frac{m_0}{\gamma_1\mp 2\gamma_2}\ , \tag{18}$$

respectively. Hence we use Eq. (3) to calculate the hole wave function with effective mass m_h^* [Eq. (18)].

Assume that the exciton envelope function $G(\rho,z)$ is a combination of Gaussian functions,

$$G(\rho,z)=\sum_{i,j} c_{ij} e^{-\alpha_i \rho^2-\beta_j z^2} . \tag{19}$$

Substituting the exciton wave function (16) and Eq. (19) into the exciton equation, we obtain the secular equation,

$$|H_{ij,i'j'}-ES_{ij,i'j'}|=0 . \tag{20}$$

where $S_{ij,i'j'}$ and $H_{ij,i'j'}$ are the overlap integrals and Hamiltonian matrix elements, respectively.

Figures 7 and 8 are the exciton binding energies as functions of well width in magnetic fields of 2, 10, and 20 T, for the heavy- and light-hole excitons, respectively. From the figures we see that when the well width increases the binding energies first increase, reach a maximum, and then decrease, approaching limited values. For the larger magnetic field the binding energy is larger, and the well width at which the binding energy reaches maximum is smaller. The binding energies of the light-hole exciton are smaller than those of the heavy-hole exciton.

The results in Figs. 7 and 8 are for the potential barrier width $B=50$ Å, which results in a strong penetration between the wells in the case of weak magnetic field. Figures 9(a) and 9(e) are the heavy-hole densities in the well width $W=100$ Å, barrier width $B=50$ Å, and magnetic fields $B=2$ and 20 T, respectively. In the strong magnetic field the hole is mainly confined in the central potential well, and the maximum binding energy occurs at smaller well width. In the weak magnetic field the holes are distributed in the central and neighbor potential wells, resulting in a decrease of the exciton binding energy. As the well width increases to a certain value, so that the holes are mainly distributed in one well, the binding energy reaches a maximum.

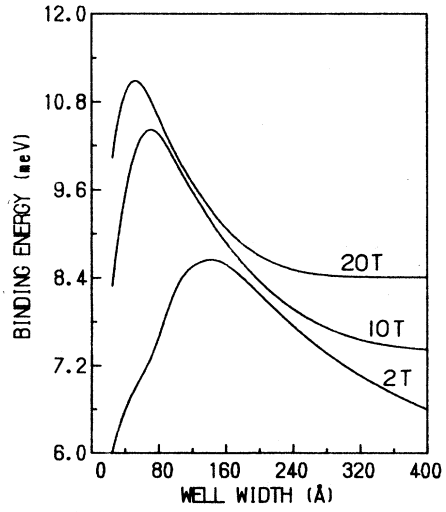

FIG. 7. Variation of binding energies of the heavy-hole exciton with the well width for three values of the magnetic field. The barrier width is 50 Å.

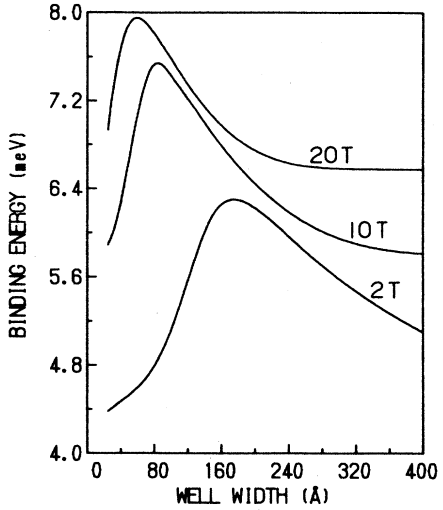

FIG. 8. Variation of binding energies of the light-hole exciton with the well width for three values of the magnetic field. The barrier width is 50 Å.

We also calculated the heavy-hole exciton binding energies in the isolated quantum wells with $B=200$ Å; the results are shown in Fig. 10. From Fig. 10 we see that the maximum exciton binding energies occur at smaller well width and are independent of the magnetic field. At larger well widths the binding energies are different for different magnetic field. Figures 9(b) and 9(f) are the heavy-hole densities at $W=100$ Å, $B=200$ Å, and mag-

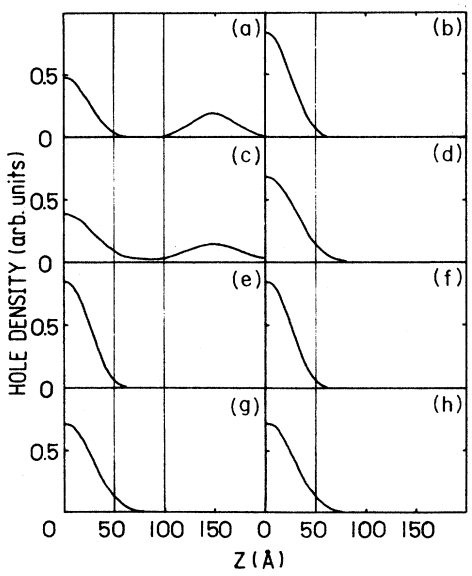

FIG. 9. Density distribution of heavy and light holes in the potential well of width 100 Å. (a)–(d), $B=2$ T; (e)–(h), $B=20$ T. (a), (b), (e), and (f), $m_h^*=0.3774m_0$; (c), (d), (g), and (h), $m_h^*=0.0905m_0$. (a), (c), (e), and (g), $B=50$ Å; (b), (d), (f), and (h), $B=200$ Å.

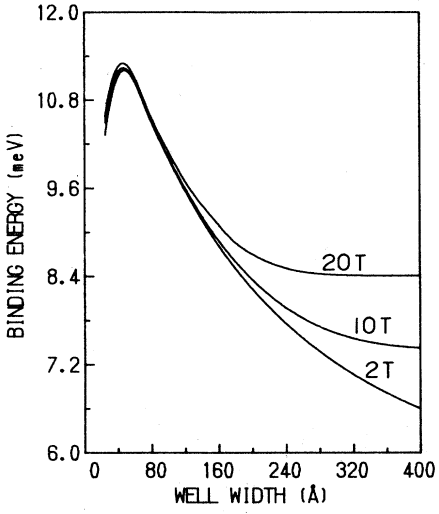

FIG. 10. Variation of binding energies of the heavy-hole exciton with the well width for three values of the magnetic field. The barrier width is 200 Å.

netic fields $B=2$ and 20 T, respectively. Comparing Figs. 9(b) and 9(f) we find that the hole densities are nearly the same for magnetic fields of 2 and 20 T, and hence the exciton binding energies are independent of the magnetic field. As the well width increases, the hole density will be different in the parabolic potential arising from different magnetic fields, resulting in the difference of the exciton binding energy.

Figures 9(c), 9(d), 9(g), and 9(h) are the corresponding results to 9(a), 9(b), 9(e), and 9(f) for the light hole. Comparing these figures, we see that the light holes spread over a larger region than the heavy holes. Therefore the exciton binding energies of light holes are smaller than those of heavy holes.

V. ELECTRONIC MAGNETIC ENERGY LEVELS IN THE MAGNETIC FIELD ALONG AN ARBITRARY DIRECTION IN THE *yz* PLANE

Chang *et al.* designed a geometry in which the magnetic field could change the direction in the *yz* plane in their magnetic-resistance measurement.[9] Using the above method, we can also calculate the electronic magnetic energy levels in this case. Let the vector potential of the magnetic field be

$$\mathbf{A}=\left[-\frac{B_z y}{2}+B_y z,\ \frac{B_z x}{2},\ 0\right], \tag{21}$$

where B_z and B_y are the components of the magnetic field along the z and y directions, respectively. The electronic Hamiltonian can be written as

$$H=\frac{1}{2m^*}[(k_x+\beta_y z)^2+k_y^2+p_z^2]+V(z), \tag{22}$$

where

$$k_x=p_x-\frac{\beta_z y}{2}, \qquad k_y=p_y+\frac{\beta_z x}{2}, \tag{23}$$

$$\beta_z=\frac{eB_z}{c}, \quad \beta_y=\frac{eB_y}{c}. \tag{24}$$

Introducing the creation and annihilation operators,

$$a^\dagger=\frac{1}{(2\hbar\beta_z)^{1/2}}(k_x+ik_y), \qquad a=\frac{1}{(2\hbar\beta_z)^{1/2}}(k_x-ik_y), \tag{25}$$

the electronic Hamiltonian (22) becomes

$$H=\frac{1}{2m^*}[2\hbar\beta_z(a^\dagger a+\tfrac{1}{2})+\beta_y(2\hbar\beta_z)^{1/2}(a+a^\dagger)z+\beta_y^2 z^2+p_z^2]+V(z). \tag{26}$$

The first term in the square brackets of (26) gives rise to the magnetic energy levels of B_z, the third and fourth terms give rise to the magnetic energy levels of B_y, and the second term represents the coupling term of B_z and B_y.

We take the wave function to be

$$\psi(\mathbf{r})=\sum_{n,m} c_{nm}u_n\varphi_m(z), \tag{27}$$

where u_n and $\varphi_m(z)$ are the wave functions of the B_z and B_y magnetic energy levels, respectively. Substituting (27) into the Hamiltonian equation (26), we can calculate the magnetic energy levels in the magnetic field along an arbitrary direction.

Figure 11 shows the electronic magnetic energy levels as functions of θ, the angle between the magnetic field

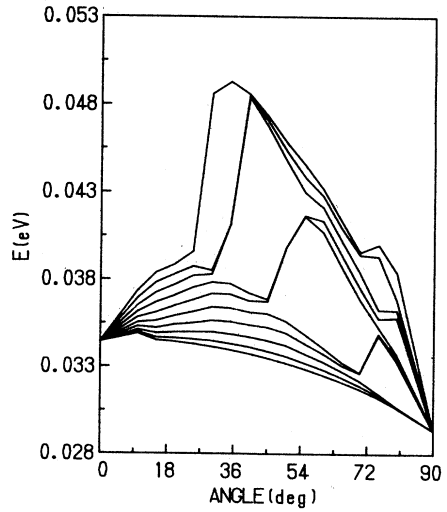

FIG. 11. Electronic magnetic energy levels as functions of the angle between the magnetic field direction and the z axis, for a magnetic field of 10 T.

and the z axis, for a magnetic field of 10 T. From Fig. 11 we see that when the magnetic field deviates from the z (or y) axis by a small angle, say $\theta=10°$ (or 80°), a band of sublevels is split out of the originally degenerate magnetic level $n=1$ associated with the magnetic field with $\theta=0°$ (or 90°) by the small B_y (or B_z) component. When the magnetic field deviates from the z (or y) direction considerably, the variations of the energy levels exhibit complicated structures. Some higher energy levels show a tendency to converge to the $n=2,3,\ldots$ excited states at $\theta=0°$ or 90°.

VI. SUMMARY

In this paper we proposed an expansion method with sine functions to study the electronic structures of superlattices in the magnetic field parallel to the interface. We studied the magnetic energy levels, optical transition matrix elements, magnetic exciton states, etc., and obtained the following main results.

(1) In the superlattices there are two kinds of magnetic energy levels for electrons and holes: one basically does not vary with z_0 (k_x) and is associated with the energy levels of superlattices without magnetic field. The other has a larger energy dispersion with z_0. The hole magnetic energy levels also exhibit energy dispersion with k_y. The density of states shows characteristics of both the two- and one-dimensional energy bands.

(2) Magnetic-optical–transition selection rules are different for transitions to the heavy- or light-hole states. For the heavy-hole states the transitions have comparable intensities for the electric field polarizations ϵ_+ (or ϵ_-) and ϵ_y. For the light-hole states there are only transitions of ϵ_+ (or ϵ_-). There are two groups of hole energy levels at $k_y=0$; the transition selection rules are also different for the two groups of hole states.

(3) The binding energy of the magnetic exciton increases with increasing magnetic field. When the well width increases, the binding energy first increases, reaches a maximum, then decreases, and approaches a constant. The well width corresponding to the maximum binding energy decreases with increasing magnetic field. The binding energy of the light-hole exciton is smaller than that of the heavy-hole exciton. The penetration between quantum wells in the case of small barrier width and weak magnetic field obviously decreases the exciton binding energy.

(4) When the direction of the magnetic field changes from the z axis to the y axis, the variation of the electronic magnetic energy levels with angle exhibits a complicated structure.

ACKNOWLEDGMENTS

This work was supported by the Chinese National Natural Science Foundation.

[1]R. L. Greene and K. K. Bajaj, Phys. Rev. B **31**, 6498 (1985).
[2]Z. Schlesinger, S. J. Allen, Y. Yafet, A. C. Gossard, and W. Wiegmann, Phys. Rev. B **32**, 5231 (1985).
[3]S. R. Eric Yang, D. A. Broido, and L. J. Sham, Phys. Rev. B **32**, 6630 (1985).
[4]D. C. Rogers, J. Singleton, R. J. Nicholas, C. T. Foxon, and K. Woodbridge, Phys. Rev. B **34**, 4002 (1986).
[5]D. C. Rogers, R. J. Nicholas, and J. C. Portal, Superlatt. Microstruct. **3**, 69 (1987).
[6]J. Z. Xiang and J. B. Xia, Acta Phys. Sin. **37**, 1915 (1988).
[7]G. Duggan, Phys. Rev. B **37**, 2759 (1988).
[8]G. E. W. Bauer and T. Ando, Phys. Rev. B **37**, 3130 (1988).
[9]L. L. Chang, H. Sakaki, C. A. Chang, and L. Esaki, Phys. Rev. Lett. **38**, 1489 (1977).
[10]L. L. Chang, E. E. Mandez, N. J. Kawai, and L. Esaki, Surf. Sci. **113**, 306 (1982).
[11]G. Belle, J. C. Maan, and G. Weimann, Solid State Commun. **56**, 65 (1985); Surf. Sci. **170**, 611 (1986).
[12]D. C. Raynolds, K. K. Bajaj, C. W. Litton, R. L. Greene, P. W. Yu, C. K. Peng, and H. Morkoç, Phys. Rev. B **35**, 4515 (1987).
[13]T. Ando, J. Phys. Soc. Jpn. **50**, 2978 (1978).
[14]J. C. Maan, in *Two-Dimensional Systems, Heterostructures and Superlattices,* Vol. 53 of *Springer Series in Solid State Sciences,* edited by G. Bauer, F. Kuchar, and H. Heinrich (Springer, Berlin, 1984), p. 183.
[15]J. C. Maan, Surf. Sci. **196**, 518 (1988).
[16]J. A. Lebens, R. H. Silsbee, and S. L. Wright, Phys. Rev. B **37**, 10 308 (1988).
[17]G. M. G. Oliveira, V. M. S. Gomes, A. S. Chaves, J. R. Leite, and J. M. Worlock, Phys. Rev. B **35**, 2896 (1987).
[18]A. Fasolino and M. Altarelli, in Band Structure Engineering in Semiconductor Microstructures, edited by R. A. Abram and M. Jaros (Plenum, New York, in press).
[19]M. Altarelli and G. Platero, Surf. Sci. **196**, 540 (1988).
[20]J. M. Luttinger, Phys. Rev. **102**, 1030 (1956).
[21]K. Hess, D. Bimberg, N. O. Lipari, J. U. Fischbach, and M. Altarelli (unpublished).
[22]L. Van Hove, Phys. Rev. **89**, 1189 (1953).